Research Article

Dual Source Solar Powered Combined-Cycle Multi-Temperature Refrigeration System for Cold Production in the Context of Off-Grid and Rural Energy Access

Didier ZEH NDOH#, Frederic LONTSI^*, Thomas DJIAKO!, Robert ZENGWA^ and Engelbert NGWA&

Accepted 25 March 2017, Available online 31 March 2017, Vol.7, No.1 (March 2017)

Abstract

It is proposed and analyzed the coupling of a dual source solar PV & T with a combined compression/ejection multitemperature refrigeration cycle intended for the simultaneous production of cold for refrigeration and freezing, in the context of off-grid and rural energy access. The developed simulation model helped to perform the system performances for environment friendly refrigerants R290, R152a and R134a. It is shown that for a 1.5 kW domestic fridge-freezer applications, using the developed system should require 4.4m² surface area PV panels and 3.1 m² surface areas solar collector; while equipping a 15kW multi-temperature cold room with this system leads to 44 m² surface area PV panels and 31 m² surface area solar collector. In addition to the effect of the incident solar irradiance, the influence of the ambient temperature on system performance was also analyzed when using a flatplate solar collector.

Keywords: Combined-cycle refrigeration system, multi-temperature, solar PV & T, coefficient of performance, off-grid and rural energy access

1. Introduction

Increasing the use of renewable in the energy mix, particularly in the field of refrigeration is essential for the decarbonization of their energy supply and use, and contributes to achieve climate and development goals. Electricity-driven refrigeration systems such as conventional vapor compression refrigeration systems are the most widely used for cold production both in refrigerating systems and in the air conditioning than thermally-driven cooling systems due to the fact that they have a high Coefficient of Performance (COP). However these installations operate with the use of electrical energy that almost results from the transformation of fossil energy resources in the thermal power plants, which results in the rejection of greenhouse gases and other pollutants in the environment.

Moreover, this type of installation is often absent or simply expensive to operate in off-grid rural areas, particularly in developing countries where precisely the populations need artificial cold for preserving perishable foodstuffs for consumption or as a source of income, even though there is an abundance of renewable energy sources such as solar and biomass.

In these conditions, the use of locally available solar energy (thermal or photovoltaic) for the production of cold for the purpose of preserving perishable foodstuffs and pharmaceuticals in rural and off-grid areas appears therefore to be a serious alternative.

Indeed, the work of Enibe (1997) for the alternative has rightly shown that solar refrigeration can play an important role in the conservation of perishable foodstuffs of rural populations in developing countries in the near future, as solar refrigeration technologies are becoming more competitive.

In the literature, several solar cooling technologies are described and classified. Kim and Infante (2008) presented a state of the art covering electricity-driven solar systems, thermally-driven solar systems and other emerging technologies together with a comparison between these technologies from the standpoint of energy efficiency and economic feasibility.

The ejection refrigeration cycles are part of solar powered cooling systems technologies. Indeed, some recent review articles (Mehdi et al., 2015) show the growing interest of researchers in these technologies over the last few years. This trend being mainly due to the number of publications related to the solar-ejector cooling systems, as recorded in the specialized journals

[#]Laboratoire d'Energétique, EDSFA/UFD SI, Université de Douala, 2701 Douala, Cameroun

[^]Faculty of Industrial Engineering, University of Douala, 3353 Douala, Cameroon

¹Institut Universitaire du Golfe de Guinée, ISTA, 12489 Douala, Cameroun

[&]amp;Department of Thermal Engineering, University institute of technology, University of Douala, 8698 Douala, Cameroon

such as the International Journal of Refrigeration (Stefan and Neal, 2016).

Integrating the ejector or its coupling to a conventional vapor compressor refrigeration system makes it possible to realize, depending on the coupling scheme, hybrid systems which considering the performance improvement that it generates, are of great interest both from the theoretical point of view and the potential applications in the multi-temperature refrigeration field (refrigeration and freezing). The refrigeration systems combining the ejector cycle and the vapor compression cycle form a family of hybrid refrigeration systems which are part of a classification elaborated by Farah et al. (2016) and which have many advantages when they are powered by solar energy. Moreover, several works on solar refrigeration have shown that systems with refrigeration cycles using an ejector and a mechanical compressor are of particular interest for both air conditioning (Sun 1997) and refrigeration (Lontsi et al., 2016).

The multi-temperature combined ejector/vapor compression refrigeration cycle proposed and investigated by Lontsi et al (2016) consists of combining an ejector refrigeration cycle with a twostage vapor compression refrigerating cycle with two evaporators, the low pressure compressor of the latter having been replaced by the ejector. The two evaporators of such a system, at different temperature levels could integrate different compartments of cold room or domestic fridge-freezer. The interest of the hybridization of such a system has been shown and solar energy is one of the energy sources identified for such an installation. However, the above mentioned study when making the system analysis did not take into account the process of converting solar radiation into the two forms of energy that can power the installation.

Furthermore, it should be noted that the electric and thermal energy needed to supply respectively the mechanical components (the compressor and pump) and the generator of such a system may be provided either by a combined solar PV & T consisting of a photovoltaic module and a solar thermal collector supplying the installation separately, or by a dual source of solar PV/T consisting of a photovoltaic module and its cooling system.

The growing number of recent research on photovoltaic-thermal systems (Xingxing et al.,2012, Joe et al.,2105, Elbreki et al., 2016) attests to the interest of these systems and their potential applications, particularly in the field of refrigeration. In fact, in some cases, the heat extracted during the cooling of the PV modules can be recovered (Joe et al., 2105). However, the temperature level of the heat extracted from the PV/T systems is generally relatively low and can only be useful for applications in the temperature range of 25-40°C (Bjornar and Rekstad, 2002) and therefore, can not allow optimum operation of the ejector of the combined cycle refrigeration system (Lontsi et al., 2016) whose temperature at the generator is supposed

to be relatively higher and above 70-80°C according to (Huang et al., 2001).

In view of the foregoing, the collector of the solar PV&T system which can produce heat at much higher temperatures, proves to be more relevant, for which reason such a hybrid solar energy source was chosen for the present study with the aim of coupling it to the combined-cycle multi-temperature system proposed by Lontsi et al. (2016) in order to analyze the global system thus constituted.

The proposed system is studied by considering applications in rural and off-grid areas in developing countries, given that the two evaporators of such a system, at different temperature levels could integrate different compartments of a cold room or a domestic fridge-freezer, taking into account local solar radiation conditions.

After introducing the system, a mathematical model is performed to determine thermodynamic performances in given conditions for selected refrigerants. Then is analyzed the influence of various chosen operating parameters on system performance characterized by the *COP*, as well as the surface areas required for the PV modules and the collector for the considered cooling capacities.

2. Description of the system

The dual source solar powered combined ejector/vapor compression refrigeration system consists of three main subsystems: The photovoltaic module intended to produce electricity, the solar collector intended to produce heat and the combined-cycle multi-temperature refrigeration sub-system which must produce cold by consuming both electrical and thermal energy provided by the two solar devices as shown in figure 1.

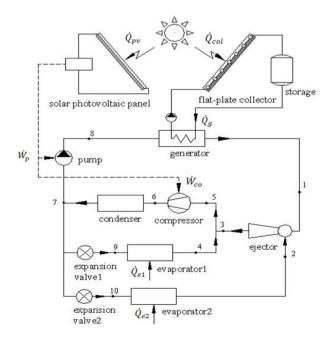


Figure 1: System principle diagram

The combined-cycle multi-temperature refrigeration system has largely been described and presented in (Lontsi et al., 2016). This hybrid system as shown in figure 1 is a combination of a power cycle (organic Rankine cycle) operating with working fluid flow rate \dot{m}_1 whose heat source is at the generator and a two-stage dual evaporator vapor compression refrigeration cycle of which the low pressure compressor has been replaced by the ejector.

The work produced by the power cycle in this case is spent in the ejector to compress the low pressure vapor from the evaporator 2 while the mechanical compressor sucks and discharges at the condensing pressure, the mixture of vapor at medium pressure coming from evaporator 1 and ejector, is at the expense of the absorbed mechanical energy from the PV sub-system. The two-stage refrigeration cycle is completed by the double expansion in the expander 1 and the expander 2 of which the refrigerant flow rates are respectively \dot{m}_4 et \dot{m}_2 .

The operation of the whole system consists of several thermodynamic transformations. At the generator, the absorbed heat from the solar collector sub-system heats up and vaporize the liquid fluid returned by the pump until obtaining superheated vapor (point 1). The obtained high pressure vapors (primary fluid) are used by the ejector for driving that coming from the evaporator 2 (point 2) and to compress them to the output (point 3) to an intermediate pressure equal to the pressure in the evaporator 1. At this point, the ejected vapors mixes with the vapor from the evaporator 1 (point 4) and the whole (point 5) is admitted to the mechanical compressor that compresses again before discharging them to the state (6) at the condensing pressure.

A fraction of the condensate obtained at point 7 with a flow rate \dot{m}_1 is sucked by the pump and discharged to the state (8), at the generator evaporation pressure while the rest will undergo expansions respectively through the expander 1 and the expander 2.

The saturated mixture coming from the expansion valve 1 with an amount \dot{m}_4 (point 9) is injected into the evaporator 1 and the remaining, whose flow rate \dot{m}_2 from the second expansion valve (point 10) is introduced into the low-pressure evaporator. After evaporation, the vapors produced in the two evaporators come out to state (4) and state (2) respectively, and the cycle starts again. The fraction of energy consumed by the pump is also provided by the PV subsystem.

3. Analysis of the dual source solar PV&T combined-cycle refrigeration system

Each of the three subsystems forming the system is modeled and, subsequently, the equations resulting from their coupling will allow analysis of the overall installation.

3.1 Combined-cycle multi-temperature refrigeration subsystem

The governing equations for analysis of the flow through every component and at mixing points of this sub-system are obtained by using principles of conservation of mass and energy in steady state as follows:

$$\sum \dot{m}_{in} = \sum \dot{m}_{out} \tag{1}$$

$$\sum \dot{Q}_i - \sum \dot{W}_i = \sum (\dot{m} h)_{out} - \sum (\dot{m} h)_{in}$$
 (2)

The ejector in particular is a key component of the combined cycle whose performance will condition that of the entire subsystem. The ejector performance is influenced by both the ejector geometry and the operating conditions (Zhu and Jiang, 2012). This performance can be evaluated in terms of the entrainment ratio ω . For optimal operation of the ejector, this ratio can be modeled by the correlation (3) as a function of pressure lift ratio and driving pressure ratio (Boumaraf and Lallemand, 1999):

$$\omega = 3.32 \left[\frac{1}{\tau} \left(1 - \frac{1.21}{\xi} \right) \right]^{2.12} \tag{3}$$

The equations for the modeling of this sub-system, based on (1) and (2) are given in detail by Lontsi et al. (2016); including expressions for evaluating superheating and sub-cooling at heat exchangers.

The combined-cycle refrigeration sub-system performance can then be measured by the coefficient of performance, defined as the ratio between the refrigeration effects to gross energy input to the cycle and calculated as follows (Lontsi et al., 2016):

$$COP_{com} = \frac{\dot{Q}_{e1} + \dot{Q}_{e2}}{\dot{W}_{co} + \dot{W}_p + \dot{Q}_g} \tag{4}$$

The mechanical and thermal powers contained in equation (4) are obtained from the application of equations (1) and (2) to the control volumes of the two evaporators, the compressor, the pump and the generator of the sub-system.

3.2 Solar photovoltaic (PV) sub-system

The photovoltaic panels are the main components of the solar electric sub-system. The incident solar radiations \dot{Q}_{pv} are converted into useful electrical energy \dot{W}_{e} , which in turn drives the mechanical compressor and the refrigerant pump of the combined-cycle refrigeration sub-system described above (figure 1). The electrical efficiency of a PV module is defined by the ratio of power output to the overall incident solar radiation.

$$\eta_{pv} = \frac{\dot{W}_e}{\dot{Q}_{pv}} \tag{5}$$

Since incident solar radiation is the product of solar panels surface area and the direct irradiation of solar beams, the following equation is given:

$$\dot{Q}_{pv} = IA_{pv} \tag{6}$$

3.3 Solar Thermal sub-system

This subsystem forms a loop consisting of a pump, solar collector, heat storage tank and generator heat exchanger as in figure 1. Solar collector is used to absorb the incident solar thermal radiation. The generated useful heat \dot{Q}_u is then used to supply the generator of the combined-cycle refrigeration system. The thermal efficiency of a solar collector is defined as the ratio of useful heat to overall incident solar radiation \dot{O}_T .

$$\eta_T = \frac{\dot{Q}_u}{\dot{Q}_T} \tag{7}$$

The overall incident solar radiation is given as a function of solar irradiation and collector's absorbing surface area, as follows:

$$\dot{Q}_T = IA_T \tag{8}$$

Flat-plate and evacuated tube (vacuum tube) are the two main types of solar collectors. The evacuated collectors (type C) with high cost have less heat lost and high performance at high temperatures while cheaper flat-plate collectors (type A) operate with low performances. According to Huang et al. (2012), by using a high-quality selective surface, good insulation design and high-performance glass cover, the flat-plate solar collector can be made with relatively high efficiency at low cost (type B). Depending on the type of selected solar collector, the efficiency can be modeled using the following equation (Huang et al., 2012):

$$\eta_T = 0.8 - C \, \frac{(T_{in} - T_0)}{I} \tag{9}$$

Where T_{in} and T_0 are the collector inlet and ambient temperature, and C, a constant depending on collector type. (C=3.5 m²W⁻¹K⁻¹; 5.7 m²W⁻¹K⁻¹ and 2 m²W⁻¹K⁻¹ for the type A, type B and type C collector respectively)

3.4 Global system

The overall system model is obtained by coupling the two solar modules to the combined cooling cycle so that the electrical energy generated by the PV module can drive the compressor and the pump, and that the solar collector can provide the heat required to operate the generator. Given the refrigerating capacity of the overall system on the two temperature levels, the overall coefficient of performance of the system is the ratio of the refrigeration effects to the total solar energy input, given as follow:

$$COP_g = \frac{\dot{Q}_{e1} + \dot{Q}_{e2}}{\dot{Q}_{mr} + \dot{Q}_T} \tag{10}$$

Considering the energy losses (electric motor losses, transmission and mechanical losses), the electrical power generated by the PV system to drive the compressor and the pump can still be written as follows:

$$\dot{W}_e = \frac{\dot{W}_{co}}{\eta_{em,co}} + \frac{\dot{W}_p}{\eta_{em,v}} \tag{11}$$

In equation (11), η_{em_co} and η_{em_p} represent respectively the electro-mechanical efficiencies of the compressor and the pump, taking into account the losses between the electrical energy generated by the PV panel and that received by the working fluid of the combined-cycle refrigeration system through these two components.

With regard to the coupling of the solar thermal sub-system with the combined-cycle refrigeration system, losses are neglected throughout the solar collector loop and, in addition, the generator is considered as a perfectly insulated counter-current heat exchanger. Under these conditions, the coupling of the two sub-systems can be modeled by the following equations:

$$\dot{Q}_u = \dot{Q}_a \tag{12}$$

$$T_{in} = T_g + \Delta T_T \tag{13}$$

Where ΔT_T is the difference between the inlet temperature of the solar collector and the generating temperature of the combined-cycle refrigeration working fluid.

Taking account of equations (4), (5), ... (12), the performances of the presented system, defined using (10), can also be given the following form:

$$COP_{g} = \eta_{emco}.\eta_{emp}.\eta_{pv}.\eta_{T}.\left[\frac{\dot{\mathbf{W}}_{co}+\dot{\mathbf{W}}_{p}+\dot{\mathbf{Q}}_{g}}{\eta_{emp}.\eta_{T}.\dot{\mathbf{W}}_{co}+\eta_{emco}.\eta_{T}.\dot{\mathbf{W}}_{p}+\eta_{emco}.\eta_{emp}.\eta_{pv}.\dot{\mathbf{Q}}_{g}}\right].COP_{com}$$

$$(14)$$

4. Computation methodology

A computer simulation model has been developed on the basis of the above equations. The calculating programs are written with Engineering Equation Solver (EES) package. The thermodynamic properties of all the considered refrigerants (R134a, R290 and R152a) are obtained from the same software data base.

The model input operating parameters are: T_{e1} , $\psi = \frac{\dot{q}_{e1}}{\dot{q}_{e2}}$, T_{e2} , \dot{Q}_{e2} , T_c , T_g . Considering super-heating $\Delta T_{e1} = \Delta T_{e2} = 5^{\circ}C$ in the two evaporators, sub-cooling $\Delta T_c = 5^{\circ}C$ in the condenser, and $\Delta T_T = 10^{\circ}C$. The isentropic efficiencies of the pump and compressor were assumed to be 0.85 and 0.8 respectively. The electrical efficiency of the PV module was assumed to be 0.16.

Thus, for the given operating conditions, ω is calculated based on equation (3) and the combined-cycle refrigeration sub-cycle thermodynamic

performance is calculated in accordance with equation (4). Thereafter, the overall performance of the proposed dual PV & T solar powered combined-cycle multi-temperature refrigeration system is evaluated by equation (10), while the photovoltaic solar panels and the solar collector surface areas are calculated by equations (6) and (8) respectively.

5. Simulation results and discussion

Based on the developed above equations of subsystems and coupling scheme, thermodynamic performances of the global system are analyzed taking into account the nature of the refrigerant, the influence of various chosen operating, climatic and design parameters.

5.1. Influence of the working fluid's nature on the system performances

The three fluids R290, R134a and R152a were adopted because it has been established (Lontsi et al., 2016) that these environmentally friendly refrigerants among 8 selected working fluids candidates for the combinedcycle multi-temperature ejector/vapor compression refrigeration cycle have the best assets as regards the valuing of low-grade heat sources over a wide range of temperature. Figure 2 illustrates the variation of system's COP with generator temperature as a function of fluid's nature. The refrigerant R290 displayed better performance followed by R152a and R134a. It can be noted for all three fluids of interest that the performance of the system over the temperature range considered at the generator does not exceed 0.26 and consequently is closer to the COP of a thermally-driven refrigeration system than that of the conventional vapor compression refrigeration system.

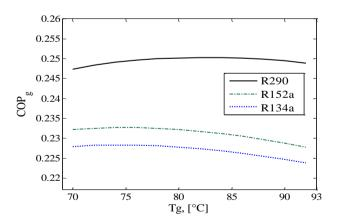


Fig.2 Variation of system's COP with T_g as a function of fluid's nature for: I=800W/m²; C=3.5m²W⁻¹K⁻¹; $T_c = 40^{\circ}C$; $\dot{Q}_{e2} = 5kW$

The fact that the adopted energy source is renewable and free of cost thus proves to be the determining factor with regard to the interest of using such a refrigeration system especially in the context of offgrid and rural energy access.

5.2 Influence of type of solar collector on the system performances

Figure 3 illustrates the evolution of the thermodynamic performances of the overall system as a function of the temperature at the generator, for the single-glazed flat-plate (C= $3.55m^2W^{-1}K^{-1}$) and the vacuum-tube (C= $2m^2W^{-1}K^{-1}$) solar collectors.

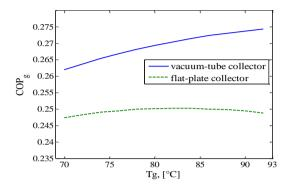


Fig.3 Variation of system's COP with T_g as a function of type of solar collector for: I=800W/m²; R290; $T_c = 40^{\circ}C; \ \dot{Q}_{e2} = 5kW$

The simulations results show that the system equipped with vacuum-tube solar collector is more efficient and that its use makes it possible to obtain a COP of the order of 0.27 when the temperature at the generator reaches 92°C. Since the study is conducted for refrigeration and freezing applications taking into account the context of off-grid and rural energy access in the developing countries, the low-cost single-glazed flat-plate solar collector although less efficient as shown in the Figure 3, is privileged for further investigations on the system.

5.3 Influence of incident solar irradiance on the system thermal efficiency

The level of incident solar radiation is part of the many climatic parameters that affect the performances of solar-based refrigeration systems (Elbreki et al., 2016). As seen from figure 4, the system overall thermal efficiency increases with increasing solar irradiance.

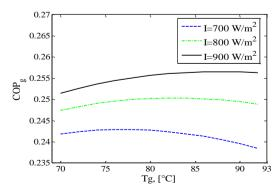


Fig.4 Variation of system's COP with T_g as a function of incident solar radiation for: C=3.5m²W⁻¹K⁻¹; R290; $T_c=40^{\circ}C;~\dot{Q}_{e2}=5kW$

This trend is explained by the fact that the efficiency of PV panels η_T is considered constant while the thermal efficiency η_T of the solar collector calculated by equation (9) increases, thereby leading to the decrease of the overall incident solar radiation \dot{Q}_T for given operating conditions and consequently the increase in system's COP.

It also appears that each curve in all the shown figures has a maximum value, which correspond to the optimum temperature at the generator, although the temperature range and simulation assumptions considered do not make it possible to bring out these optimums for all curves

5.4 Influence of the condensation temperature on the COP of the system

To account for the influence of ambient temperature on the thermodynamic performance of the system, a simulation of the operation of the installation has been carried out by varying the condensation temperature T_c from 40°C to 50°C as shown in figure 5. This temperature range corresponds to applications in harsh climatic conditions. The increase of the condensing temperature leads to a decrease of system's COP as shown in figure 5. Increasing the condensing temperature leads to an increase in the compression ratio of the mechanical compressor, while that of the ejection cycle remains unchanged. However it appears that under the same conditions, the thermal efficiency of the solar collector increases slightly with the increase in condensation temperature, resulting in a slight decrease in \dot{Q}_T (a decrease of about 3.8% when T_c from 40°C to 50°C). But since the decrease in performance of the cycle due to the increase of the condenser temperature leads to a sharp rise in \dot{Q}_{pv} (about 24.6% when T_c from 40°C to 50°C), it follows that the overall COP of the system decreases (about 3.6%) in accordance with the equation (10) despite the two opposite trends mentioned regarding the performance of the combined refrigeration cycle and the thermal efficiency of the solar collector.

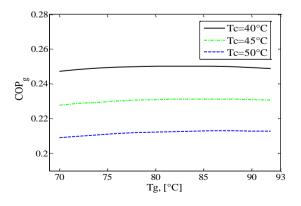


Fig.5 Influence of temperature T_C on system performances: I=800W/m²; R290; C=3.5m²W-¹K-¹; $\dot{Q}_{e2}=5kW$

5.5 Variation of PV module and collector surface areas depending on the field of use of the generated cooling capacities

The dual PV & T solar driven combined-cycle multitemperature compression/ejection refrigeration system intended for the simultaneous production of cold for refrigeration and freezing is developed mainly for developing countries in the context of off-grid and rural energy access. Even if the system is supplied by a cost free energy source, the cost of such an installation depends on the value of the surface areas of both PV module and solar collector. Simulations of the developed model were done as regards these surface areas as depicted in Figure 6 in order to analyze and identify the practical interest of such a hybrid system.

Figure 6a shows the evolution of these surface areas as function of generator temperature T_g when the installation functions as a domestic fridge-freezer with cooling capacities of respectively 0.5kW for freezing and 1kW for refrigeration, whereas figure 6b illustrates the evolution of the same surface areas when the system is assumed to equip a multitemperature cold room having the cooling capacities of 5kW for the negative cold and 10kW for the positive cold respectively.

In both application cases it is observed that the surface area of PV module A_{pv} decreases when increasing T_g while the surface area of the solar collector A_T increases with T_q . In addition, A_{pv} remains greater than A_T in the considered temperature range for T_a . The ejector driving pressure ratio increases with increasing T_g , which results in an increase in the COP of the combined-cycle. But since the increase in performance of the cycle (due to the increase of the ejector entrainment ratio) leads to the reduction of the electric power necessary to operate the mechanical compressor, it follows the observed decrease in the surface area of the PV module. On the other hand, the increase in T_q leads to the decrease in the thermal efficiency of the solar collector according to equation (9). This results in an increase in heat input to the generator, which explains the observed increase in the surface area of the solar collector. Finally, in the temperature range considered for T_q , the values obtained for A_{pv} and A_T are acceptable from the practical point of view as regards the operation of the system as a domestic fridge-freezer on the one hand and its operation in a multi-temperature cold room on the other hand, based on the above-mentioned cooling capacities. On average, these surface areas are respectively $(A_{pv} = 4.4m^2; A_T = 3.1m^2)$ for the domestic applications and $(A_{pv} = 44m^2 ; A_T = 31m^2)$ for the multi-temperature cold room.

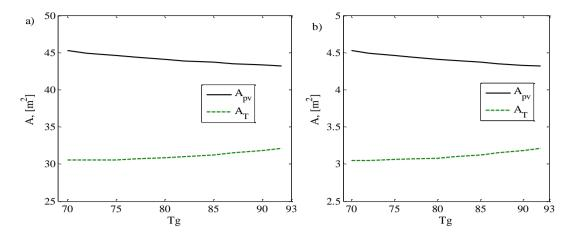


Fig.6 Variation of PV and collector surface areas with T_g for: $I=800W/m^2$; R290; $\psi=2$; $T_c=40$ °C; $C=3.5m^2W^{-1}K^{-1}$ a) The system equips a cold room with $\dot{Q}_{e2}=5kW$.

b) The system functions as a domestic fridge-freezer with $\dot{Q}_{e2}=0.5kW$.

Conclusion

The coupling of a solar PV & T energy source with a combined-cycle multi-temperature compression/ ejection refrigeration cycle was performed. Based on the developed model, the thermodynamic analysis of the system which includes a dual hybridization with regard to the energy source and the refrigeration cycle showed its interest in valuing the solar energy especially in the context of off-grid and rural energy access in developing countries for local community cold room applications.

It is shown that for all three fluids of interest, the overall COP of the system is closer to the COP of a thermally-driven refrigeration system than that of a typical conventional vapor compression refrigeration system. Generally, the thermodynamic performance of the system increases with the increase of incident solar radiation but decreases when the ambient temperature increases.

In addition, even using the low-cost single-glazed flat-plate solar collector makes it possible to achieve 1.5 kW cooling capacity for a domestic fridge-freezer applications with only $4.4m^2$ surface area PV panels and $3.1m^2$ surface areas solar collector. The surface areas required to operate a 15kW multi-temperature cold room with such a system under the same conditions would be about $44m^2$ for PV panels and $31m^2$ for solar collector respectively.

Acknowledgements

The authors would like to acknowledge the Ministry of Higher Education of Cameroon for providing financial support to this work.

References

S.O. Enibe (1997). Solar refrigeration for rural applications. *Renewable energy*. Vol.12, No.2167

D S Kim, C A Infante Ferreira (2008). Solar refrigeration options-a state-of-the-art review. *International Journal of Refrigeration*. 3, pp13-15.

Mehdi Zeyghami, D.Yogi Goswami, Elias Stefanakos (2015). A review of solar thermo-mechanical refrigeration and cooling methods. *Renewable and Sustainable Energy Reviews*. 51, pp1428–1445.

Stefan Elbel, Neal Lawrence (2016). Review of recent developments in advanced ejector technology. *International Journal of Refrigeration*. 62, pp1-18.

Farah Kojok, Farouk Fardoun, Rafic Younes, Rachid Outbib (2016). Hybrid cooling systems: A review and an optimized selection scheme. *Renewable and Sustainable Energy Reviews*. 65, pp57–80

Sun DW (1997). Solar powered combined ejector-vapor compression cycle for air conditioning and refrigeration. *Energy Conversion and Management*. 38, pp479-491.

F. Lontsi, O. Hamandjoda, O. T. Sosso Mayi, A. Kemajou (2016). Development and performance analysis of a multi-temperature combined compression/ejection refrigeration cycle using environment friendly refrigerants. *International Journal of Refrigeration*. 69, pp 42-50.

Xingxing Zhanga, Xudong Zhaoa, Stefan Smitha, Jihuan Xub, Xiaotong Yuc (2012). Review of R&D progress and practical application of the solar photovoltaic/thermal (PV/T) technologies. *Renewable and Sustainable Energy Reviews*. 16, pp599–617.

Joe Joe Michael, Iniyan S, Ranko Goic (2015). Plat plate solar photovoltaic –thermal (PV/T) systems: A reference guide. *Renewable and Sustainable Energy Review.* 50, pp 62-88

A.M. Elbreki, M.A. Alghoul, A.N. Al-Shamani, A.A. Ammar, Bita Yegani (2016). The role of climatic-design-operational parameters on combined PV/T collector performance: A critical review. *Renewable and sustainable Energy Review*. 57, pp602-647

Bjornar Sandnes, John Rekstad (2002). A photovoltaic/thermal (PV/T) collector with a polymer absorber plate. Experimental study and analytical model. *Solar Energy*. 72, pp 63-73.

B.J. Huang, W.A. Petrenko, I.YA. Samofatov and N.A. Shchetinna (2001). Collector selection for solar ejector cooling system. *Solar energy*. 7,1 pp269-274.

Nomenclature

A surface area, [m²]

h enthalpy, [J.kg⁻¹]I solar irradiation [W.m⁻²]

 \dot{m} mass flow rate, [kg.s⁻¹]

P pressure, [Pa]

 \dot{Q} thermal power, [W]

T temperature, [°C]

 \dot{W} power, [W]

Greeks symbols

 ΔT superheat, subcooling, [°C]

 η efficiency

 ξ driving pressure ratio

pressure lift ratio or ejector compression ratio

 ψ cooling capacity ratio

 ω entrainment ratio

Subscripts

1,2,3.. state or points of cycle

condenser, collector

co compressor

com combined-cycle

e evaporator, electrical

g generator, global, overall

p pump

pv photovoltaic or solar electrical

T refers to solar thermal